Accurate and unbiased estimation of power-law exponents from single-emitter blinking data

Jacob P. Hoogenboom[a)]
Optical Techniques, Faculty of Science and Technology, MESA+ Institute for Nanotechnology, University of Twente, P.O. Box 217, NL-7500 AE Enschede, The Netherlands

Wouter K. den Otter
Computational Biophysics, Faculty of Science and Technology, University of Twente, P.O. Box 217, NL-7500 AE Enschede, The Netherlands

Herman L. Offerhaus
Optical Techniques, Faculty of Science and Technology, MESA+ Institute for Nanotechnology, University of Twente, P.O. Box 217, NL-7500 AE Enschede, The Netherlands

(Received 27 July 2006; accepted 6 October 2006; published online 29 November 2006)

Single emitter blinking with a power-law distribution for the on and off times has been observed on a variety of systems including semiconductor nanocrystals, conjugated polymers, fluorescent proteins, and organic fluorophores. The origin of this behavior is still under debate. Reliable estimation of power exponents from experimental data is crucial in validating the various models under consideration. We derive a maximum likelihood estimator for power-law distributed data and analyze its accuracy as a function of data set size and power exponent both analytically and numerically. Results are compared to least-squares fitting of the double logarithmically transformed probability density. We demonstrate that least-squares fitting introduces a severe bias in the estimation result and that the maximum likelihood procedure is superior in retrieving the correct exponent and reducing the statistical error. For a data set as small as 50 data points, the error margins of the maximum likelihood estimator are already below 7%, giving the possibility to quantify blinking behavior when data set size is limited, e.g., due to photobleaching. © *2006 American Institute of Physics*. [DOI: 10.1063/1.2387165]

I. INTRODUCTION

In the past 20 years single-molecule spectroscopy has become an important tool in physics, chemistry, and biology.[1] One of the defining and intriguing observations on single emitters is a pronounced blinking behavior:[2] the fluorescence or luminescence intensity of almost any type of single emitter is found to randomly switch off and on despite continuous excitation.[3–9] In general, this emission intermittency is the result of temporary excursions from the excited state to a dark state from which the excited electron returns to the ground state via a nonradiative pathway.[10] A well-known and intensively studied example is the symmetry forbidden population and depopulation of the triplet state in organic fluorophores.[3,11,12] This triplet blinking results in a single-molecule intensity trace interrupted by off periods with a typical duration of several milliseconds. In this case the durations of on and off periods each follow a single-exponential distribution. The averages of both distributions are the triplet lifetime and the intersystem crossing yield, respectively.

On/off intermittency with a much broader range of on and off period durations was first observed on fluorescent proteins[4] and multichromophore conjugated polymers[5] and was later intensively studied on single semiconductor nanocrystals and quantum dots.[6–8,13–17] Here, the distribution of on and off times, ranging from milliseconds up to hundreds of seconds, was found to follow a power-law $\sim t^{-\alpha}$ behavior, with $\alpha > 1$. Several implications of the occurrence of such a power-law distribution are as follows: (i) there is finite probability of observing an on or off period with a duration as long as the measurement time, (ii) average on or off times are not defined, and (iii) the system behaves nonergodic, i.e., the result of time-averaging single-emitter data does not equal ensemble averaging.[18,19] Recently, this power-law blinking has also been observed for the emission intensity of fluorescent organic molecules.[9,12,20]

For both semiconductor nanocrystals[7,13,15,21] as well as for organic molecules,[9,22] the occurrence of power-law blinking is generally ascribed to a charge separation reaction. When the emitter switches off, it is in a charged state that either does not absorb the excitation light or that follows a nonradiative pathway. The ejected electron or hole is trapped by a charge acceptor in the environment. How this charge separation reaction exactly results in power-law distributed on and off periods is under debate. Several models discuss the power-law behavior in terms of (i) one-dimensional spectral diffusion of charge donor and acceptor energy levels,[7,23] (ii) charge separation and recombination controlled by three-dimensional spatial diffusion of charge acceptors,[24] (iii) electron or hole tunneling from the excited state to a spatial distribution of acceptors,[13,15,25] or (iv) the formation of mul-

[a)]Author to whom correspondence should be addressed. Electronic mail: j.p.hoogenboom@tnw.utwente.nl

tiple localized excitons that each have competing pathways for charge recombination.[26] The differences between these models are evidenced in different predictions for the observed power-law exponent α. For instance, α can be expected to show a universal value of 1.5 [models (i), (ii), and (iv)],[7,23,24,26] may be environment dependent [models (ii) and (iii)], related to charge tunneling barriers [model (iii)],[13,15,25] or dependent on the dielectric properties of the medium in which the emitter is embedded [models (ii) and (iii)].[17,24] Clearly, the experimental determination of the precise value for the power exponent on the level of single emitters is crucial in understanding the nature of power-law blinking.

Several techniques exist to retrieve the power exponents governing the blinking of single emitters. These include calculation of the intensity correlation function,[27] determination of the power spectral density of intensity fluctuations,[28] and direct evaluation of the distributions of on- and off-time durations.[6] The latter technique is most commonly used and has the advantage that it assesses the on and off kinetics separately. Assessment of the power-law behavior requires an evaluation of the functional form of either intensity correlation function, power spectral density, or on- and off-time duration probability densities over multiple orders of magnitude in time. Usually this is done by performing a double logarithmic (log-log) transformation followed by least-squares (LS) fitting in which the power exponent α is determined. The combined use of a log transformation and LS is, however, known to introduce bias in the fitting result.[29–31] Recently, Stefani *et al.* have noted this discrepancy between the power exponent that was put into simulated blinking traces and the one retrieved from those traces with LS.[16] They then retrieved power exponent estimates by comparing the experimental results to the outcome of iteratively performed simulations with known power exponent. A direct, unbiased estimation method has not yet been identified, nor have the error margins involved in the estimation techniques been evaluated.

Maximum likelihood estimation (MLE) is a general estimation routine that involves calculation of the likelihood that a data set is drawn from a model distribution characterized by a certain parameter.[32] Maximization of the likelihood with respect to this parameter yields the best estimation for this model parameter. MLE has previously been shown to be a more reliable estimation routine than LS for evaluating the single-exponential (log-linear) relation for single-molecule fluorescence lifetime data.[29,30,33] Also for various other problems in single-molecule physics, MLE has appeared as a robust estimation routine[34] that can overcome a bias, e.g., when data are bound to physical constraints.[35] In the case of evaluation of on- and off-time distributions, MLE has the further advantage that it can be performed directly on the data, while LS requires additional binning in the construction of on- and off-time histograms. Note that if measurement errors are normally distributed for all data points, LS can be derived as a special case of MLE.[32] However, the log-log transformation together with a low number of events per bin distorts the measurement errors unequally.

Recently, MLE has been suggested as an estimation procedure superior to LS in assessing power-law data.[31] To our knowledge, the MLE technique has not yet been used for quantifying blinking data and the statistical errors involved in both MLE and in LS fitting have not yet been addressed. This information is crucial in validating the various models for single-emitter blinking, especially where one needs to evaluate whether single-emitter exponents are universal or exhibit a broad distribution of values. The size dependence of the accuracy of estimation routines is particularly important in the recently reported case of single-molecule fluorescence blinking,[9,12,20,36] where photoinduced bleaching poses a severe restriction on data set size.

In this article, we compare the accuracy and applicability of LS and MLE algorithms for estimation of power exponents in single-emitter blinking data and we assess the reliability of both techniques as a function of data set size. Our results demonstrate that LS introduces a severe bias that is not present in the MLE procedure. This bias in the LS can be overcome by applying a logarithmic binning in the construction of the on- or off-time histogram. However, the MLE algorithm is superior in statistical accuracy and can be performed in a computationally simple and fast way directly on the sequence of on or off times. With MLE the power exponent can be reliably estimated up to the first decimal for data sets containing as few as 50 events and power exponent $\alpha \sim 1.5$. We evaluate the accuracy and statistical error of the MLE procedure as a function of α both analytically and numerically. Finally, we will discuss an easy computational procedure that can be used in combination with MLE to discriminate power-law behavior against, e.g., single-exponential behavior without the need for graphical inspection of the data distribution. The results presented here are essential for assessing the homo- or heterogeneity of power exponent distributions of single luminescent nanocrystals or fluorescent molecules. Furthermore, MLE can be used to check for possible dynamic effects[37] by evaluating power exponents over small subsets within a single-emitter data set.

The remainder of this paper is organized as follows: First, we briefly illustrate single-emitter blinking and the occurrence of power-law blinking. Then the MLE procedure is summarized and the derivation of the likelihood function for a power-law distribution is presented. For the MLE estimator we derive analytical expressions for the average estimator retrieved from a finite-size data set and for the standard deviation, or statistical error, on this estimator. The details of the calculations used to compare MLE and LS are described in Sec. IV. Section V, containing the results and discussion of the evaluation of the two estimation routines for power-law data, is divided into three parts. First, we compare LS techniques with the MLE method for different data set sizes. Then the accuracy and statistical error margins involved in the MLE method will be investigated in detail as a function of both data set size and power exponent. Finally, we will discuss the assessment of whether or not data actually follow a power-law behavior and an easy to use computational test that can for this purpose be used in combination with MLE is presented. All results are summarized together with some concluding remarks in Sec. VI.

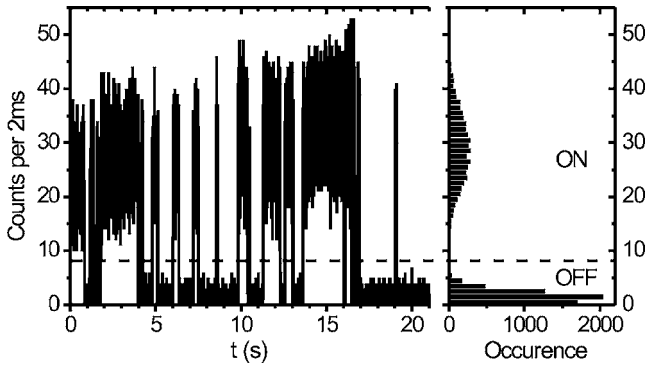

FIG. 1. Example of an intensity trace of a blinking fluorophore (left). The emission of fluorescence photons is interrupted by intervals of varying duration where the intensity falls to the background level. Based on the distribution of detected photon counts per time bin (right), a threshold is defined that separates on and off periods.

II. SINGLE-EMITTER BLINKING

The occurrence of power-law distributed on/off blinking in semiconductor nanocrystals and recently in organic fluorophores has been previously described in detail.[6–9,12–18,20] In Fig. 1, we present an example of an intensity trajectory of a blinking fluorophore. The molecule under investigation, a tetraphenoxy-perylene diïmide dye, was under continuous illumination with 10 kW/cm^2 at a wavelength of 568 nm from an ArKr laser.[36] Photons were collected per time bin of 2 ms and we observed an emission level of approximately 30 counts/2 ms. The stream of photons is, however, repeatedly interrupted; the emission intensity drops to the background level and jumps back to the emission level at a later time. The periods that the trace spends at the background level vary from the time bin to several seconds. This behavior persists when zooming in or out to smaller or larger time scales.[6,36]

The kinetics of this blinking behavior can be retrieved from the intensity trace by determining the durations of all on and off periods occurring in the intensity trace. Similarly, one can evaluate the intensity correlation function,[27] but by analyzing on- and off-time durations both on-to-off and off-to-on kinetics can be evaluated separately. Based on a histogram of the number of photon counts per time bin (see Fig. 1), a threshold can be defined that separates the emissive state from the background level.[12,38] Thus, the intensity trace is divided in a sequence of on and off states of varying duration. From the series of on and off times, the probability density for the occurrence of a specific on or off time can be calculated.

In Fig. 2 we show the probability densities for the off-period and on-period durations for the molecule in Fig. 1. Both quantities are displayed on double logarithmic axes and can be seen to span a broad range of decades on both axes. We observe a clear log-log dependence of the probability density for both off- and on-time durations, as indicated by the straight lines. Thus, both probability densities obey a power law $\sim t^{-\alpha}$ behavior, where the power exponent α may be different for the off times compared to the on times. In the remainder of this paper, we will be concerned with the determination of α from experimental data.

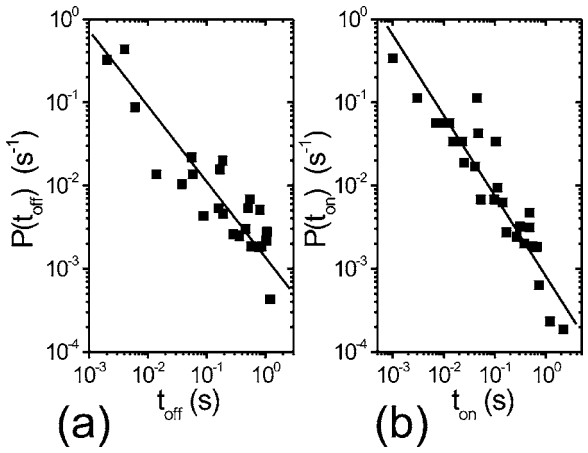

FIG. 2. Probability density for (a) the duration of the off states and (b) the duration of the on states for the fluorophore timetrace depicted in Fig. 1. The straight lines have been drawn to indicate the log-log dependency of the data corresponding to power-law behavior.

III. THE MLE ALGORITHM

Maximum likelihood estimation has been described before in relation to problems such as analyzing single-exponential lifetime data,[29,30,33] polarization modulation data,[34] and constrained single-molecule data.[35] Here, we are concerned with extracting the power exponent from power-law distributed data and as such we will limit our description to the implementation of the MLE procedure for this case. The power-law distributed probability is characterized by a prefactor A and a model exponent α,

$$P(t) = At^{-\alpha}. \tag{1}$$

A measurement yields a finite set of N discrete data points $\{t_i\}$, with $i=1,\ldots,N$. Here, the $\{t_i\}$ are the sets of observed on or off times in a single-molecule trace. The observable range of data points is limited by the experimental time resolution $t_{\min}$ and the time window of the experiment, $t_{\max}$. The prefactor A is set by requiring normalization,

$$\int_{t_{\min}}^{t_{\max}} P(t)dt = 1. \tag{2}$$

Thus, we get for Eq. (1)

$$P(t) = \frac{\alpha - 1}{t_{\min}^{1-\alpha} - t_{\max}^{1-\alpha}} t^{-\alpha}. \tag{3}$$

The likelihood function L in terms of the model parameter α is constructed by multiplying the probabilities of all data points t_i,

$$L(\alpha) = \prod_i P(t_i|\alpha). \tag{4}$$

The best estimate for α given the data set $\{t_i\}$ can now be retrieved by maximizing L with respect to α. This maximization is equivalent to maximizing the logarithm of L, so we can take

$$\left(\frac{\partial \ln L(\alpha)}{\partial \alpha}\right)_{\alpha=m} = 0. \tag{5}$$

Here and in the remainder of this paper, we use α to denote the model power exponent and m for the best estimation given the data set $\{t_i\}$. Using Eqs. (3) and (4), Eq. (5) can be rewritten as

$$\frac{1}{N}\sum_{i=1}^{N} \ln(t_i) = \left(\frac{\partial}{\partial \alpha} \left\{ \ln\left(\frac{\alpha - 1}{t_{\min}^{1-\alpha} - t_{\max}^{1-\alpha}} \right) \right\} \right)_{\alpha = m}. \tag{6}$$

Now, on the left-hand side of Eq. (6), we encounter a simple summation over all data points $\{t_i\}$. Performing the differentiation on the right-hand side and presuming $m \neq 1$ lead to

$$\frac{1}{N}\sum_{i=1}^{N} \ln(t_i) = \frac{1}{m-1} + \frac{[\ln(t_{\min}) t_{\min}^{1-m} - \ln(t_{\max}) t_{\max}^{1-m}]}{t_{\min}^{1-m} - t_{\max}^{1-m}}. \tag{7}$$

In general, the experimental time window spans several orders of magnitude so that $t_{\max} \gg t_{\min}$. Scaling all t_i with $t_{\min}$, taking $t_{\max}/t_{\min} \to \infty$, and $m > 1$, we have

$$\begin{aligned} m &= 1 + \frac{1}{S}, \\ S &= \frac{1}{N}\sum_{i=1}^{N} \ln\left(\frac{t_i}{t_{\min}} \right). \end{aligned} \tag{8}$$

Equation (8) shows that the maximum likelihood estimate m for the power exponent α can be obtained by a simple summation over all individual data points. No binning, e.g., to build a histogram or probability density, is necessary. Thus, the MLE estimate for α can be retrieved in a simple and computationally fast way from the series of on or off times.

Now, we are interested in the accuracy and statistical error contained in the MLE result in Eq. (8) as a consequence of the use of a finite N-sized data set. We have seen in Eq. (8) that the information retrieved from the data series is contained in the factor S, which is simply the expectation value $S = \langle \ln(t_i/t_{\min}) \rangle$. Calculation of $\langle \ln(t_i/t_{\min}) \rangle$ over a power-law probability density with exponent α yields the obvious result

$$\langle S \rangle = \frac{1}{\alpha - 1}. \tag{9}$$

Similarly, we can calculate the second order moment for S for which we find $\langle S^2 \rangle - \langle S \rangle^2 = (\alpha - 1)^{-2}$. For a data set consisting of N data points $\{t_i\}$, we thus have for the standard deviation of S

$$\sigma_S = \frac{1}{(\alpha - 1)\sqrt{N}}. \tag{10}$$

We are interested in the expectation value $\langle m \rangle$ and the standard deviation σ_m. A single measurement yields a series of N data points $\{t_i\}$, from which the value S_j is calculated according to Eq. (8). Thus, with S_j we denote the outcome of a single measurement on a system characterized by power exponent α. Performing multiple measurements on the same system and averaging over all measured S_j result in the average $\langle S \rangle$ given in Eq. (9). Now, the S_j will deviate from the average $\langle S \rangle$ with standard deviation σ_s given in Eq. (10), and we write $S_j - \langle S \rangle = dS$. Note that $\langle (dS)^2 \rangle = \sigma_s^2$. With S_j, we calculate the power exponent estimate m_j, for which we have $m_j - \langle m \rangle = dm$. With $m_j = 1 + 1/S_j$ we find

$$\langle m \rangle + dm = 1 + \frac{1}{\langle S \rangle + dS}. \tag{11}$$

For the last term on the right-hand side of Eq. (11) we can perform a Taylor expansion around $\langle S \rangle$,

$$\frac{1}{\langle S \rangle + dS} = \frac{1}{\langle S \rangle} - \frac{dS}{\langle S \rangle^2} + \frac{(dS)^2}{\langle S \rangle^3} + \text{h.o.t.} \tag{12}$$

Here, h.o.t. stands for higher order terms. Now, we can find the expectation value for m by averaging over all possible dS and using $\langle dS \rangle = 0$,

$$\langle m \rangle = 1 + \frac{1}{\langle S \rangle} + \frac{\langle (dS)^2 \rangle}{\langle S \rangle^3} + \text{h.o.t.} \tag{13}$$

Combining Eq. (13) with the results in Eqs. (9) and (10) and neglecting all terms of order four and higher, we arrive at

$$\langle m \rangle = \alpha + \frac{\alpha - 1}{N}. \tag{14}$$

Furthermore, insertion of Eqs. (12) and (13) into Eq. (11) yields an expression for dm, which, after squaring, averaging, and again neglecting higher order terms, leads to

$$\langle (dm)^2 \rangle = \frac{\langle (dS)^2 \rangle}{\langle S \rangle^4}. \tag{15}$$

Using Eqs. (9) and (10), and $\sigma_m^2 = \langle (dm)^2 \rangle$, we arrive at an expression for the standard deviation of the power exponent estimate retrieved from an N-sized data set,

$$\sigma_m = \frac{\alpha - 1}{\sqrt{N}}. \tag{16}$$

Now, in Eqs. (14) and (16) we have expressions for the accuracy of the maximum likelihood estimate m, and its statistical error margin σ_m. We can see from Eq. (14) that the maximum likelihood estimator m defined in Eq. (8) very well approximates the true exponent α, but with an overestimation that is inversely proportional to the number of measured data points. Furthermore, the statistical error in the MLE result exhibits the usual $1/\sqrt{N}$ dependency.

IV. CALCULATIONS

In order to evaluate and compare the accuracy of the MLE and LS techniques, both procedures were applied on sets of data points following a power-law distribution with known power exponent. To this end, we started with a series of random numbers $\{x_i\}$, uniformly distributed over the interval $\langle 0, 1]$. The random numbers were generated using either a random number generator or atmospheric noise.[39] Both procedures yielded similar results. The data series $\{x_i\}$ was transformed to a power-law $t^{-\alpha}$ distributed series by taking[32]

$$t = x^{1/(1-\alpha)}. \tag{17}$$

As in Eq. (5), we will use α to denote the power-law exponent input to the transformation, which thus is the "ideal" model power exponent. Similarly, the estimates retrieved from the finite series of random numbers will be denoted by the symbol m. Note that after the transformation in Eq. (17), we have $t_{\min}=1$.

For evaluation of the MLE procedure a series of in total $N_{\text{tot}}=10^5$ random numbers was drawn from a power-law distribution with exponent α using Eq. (17). The estimator m_{MLE} was then calculated according to Eq. (8). To investigate the accuracy of m_{MLE} as a function of data size N, the total series was divided into N_{tot}/N subseries of size N. For each subseries m_{MLE} was calculated. One of the advantages of the MLE procedure is that it can be performed directly on the sequence of on and off times. In an experimental situation, however, all data are usually binned in terms of the time resolution $t_{\min}$. Both these situations will be compared and we will refer to the MLE result on the sequence generated using Eq. (17) as the "exact times" result. The binning was performed by rounding the exact times series to the nearest integer multiple of $t_{\min}$ and these will be denoted as the "binned times."

The LS procedure was similarly evaluated as a function of N using a master series of $N_{\text{tot}}=10^6$. The procedure for extracting m_{LS} is illustrated in Fig. 3(a). First, a frequency histogram is constructed and normalized to assess the measured probability for the occurrence of a specific time in the N-sized data set. As can be seen in Fig. 3(a), the long range of the power-law distribution leads to a three order of magnitude tail in the histogram with single encounters. The power-law exponent can now be assessed by introducing an (arbitrary) cutoff to remove the single-event bins from the histogram and analyzing the linear regime only, but the statistical information contained in these rare events can better be used by calculating the corresponding probability density, i.e., scaling the histogram data to the surrounding interval in which there was no event.[13] Clearly, from the probability density in Fig. 3(a), the power-law dependency and the full range of the data set are immediately evident. The LS estimator for the power exponent is now retrieved by least-squares fitting of the log-log transformed probability density depicted in Fig. 3(a).

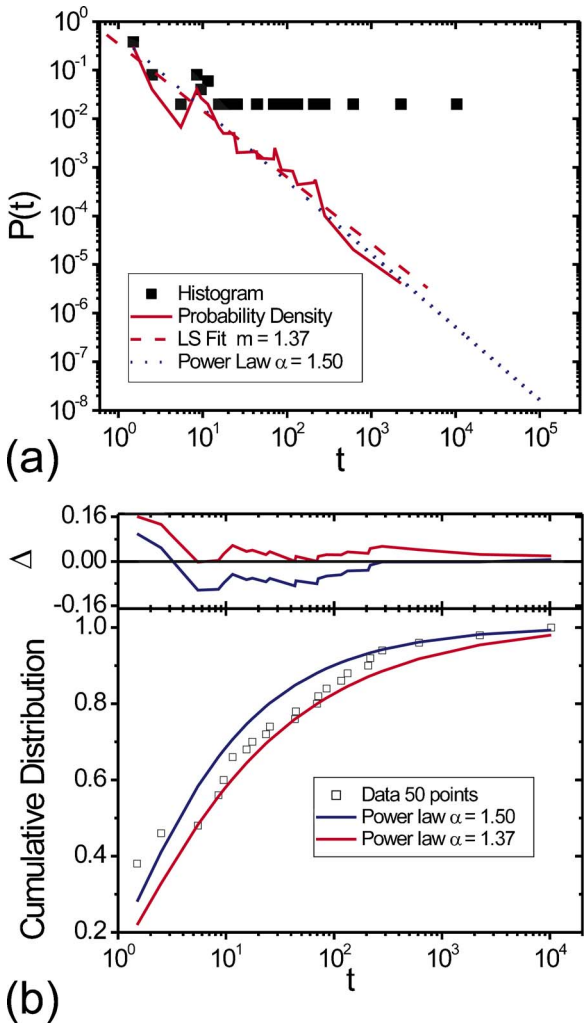

FIG. 3. (Color online) (a) Histogram and corresponding probability density for a sequence of 50 data points drawn from a power-law distribution with $\alpha=1.5$. The dashed red line is the result of a least-squares fit of the probability density ($m=1.37$); and the dotted blue line indicates an $\alpha=1.5$ power law. The bottom panel in (b) displays the cumulative distribution for the data series in (a) (open squares) together with the cumulative distributions for power laws with $\alpha=1.5$ (blue solid line) and $\alpha=1.37$ (red dashed line). The top panel gives the difference Δ between the data cumulative distribution and both power-law cumulative distributions.

V. RESULTS AND DISCUSSION

A. Comparison between MLE and LS

Using the procedure outlined before, we have assessed the accuracy of the MLE and LS procedures in reproducing model power exponents as a function of data set size. In Fig. 4, we plot the distribution of power exponent estimators as a function of data set size for both methods. In both cases, the underlying power exponent had a value of $\alpha=1.5$. For every value of data set size N, the distribution of m_{LS} can be seen to be markedly broader than the distribution of m_{MLE}. Even more important, whereas the distribution of m_{MLE} is correctly centered around $m_{\text{MLE}}=1.5$ for every N, the distribution for m_{LS} is seen to be shifted towards $m_{\text{LS}}=1.4$ for all values of N. Thus, the LS procedure underestimates the actual value of the power exponent. This underestimation persists even up to $N=10^5$, for which we find a MLE estimator of $m_{\text{MLE}}=1.502$. The LS result over the entire data series gives $m_{\text{LS}}=1.42$ for $N=10^6$ indicating persistent underestimation. Furthermore, for exponents differing from $\alpha=1.5$, similar underestimation in the LS estimator is found. For instance, for $\alpha=1.2$ and $\alpha=1.7$, we find $m_{\text{LS}}=1.14$ and $m_{\text{LS}}=1.58$, respectively, with $N=100$ and averaged over 1000 data sets.

In the example that we have given on the LS procedure in Fig. 3(a), the underestimation is also apparent: LS fitting of the log-log transformed probability density gives an estimator of $m_{\text{LS}}=1.37$, compared to an input value of $\alpha=1.50$. We can compare the data set to both the power-law models with $\alpha=1.50$ and $\alpha=1.37$, respectively, by looking at the cumulative distributions [Fig. 3(b)]. This procedure is known as the Kolmogorov-Smirnov test, which is commonly used to test the equivalence of two data sets or a data set and a model.[32] The cumulative distribution gives, for every value of t, the fraction of data points with a value smaller than or

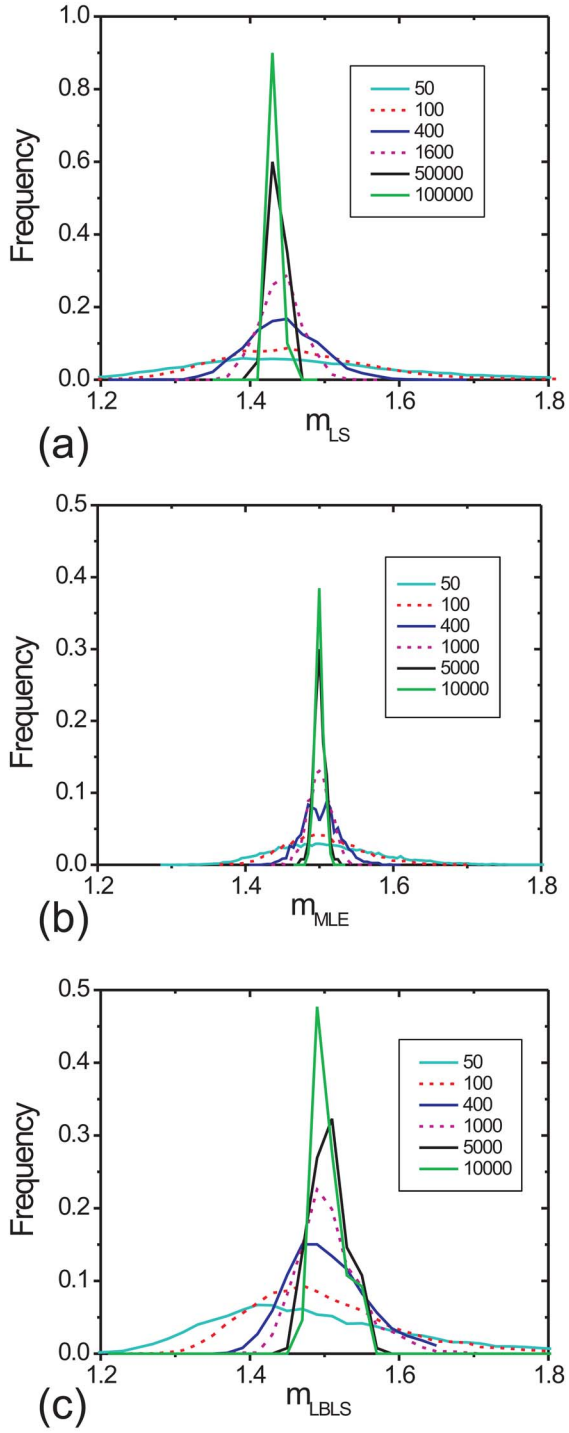

FIG. 4. (Color online) (a) Distribution of the power exponent estimators retrieved via least-squares (LS) fitting of the log-log transformed probability distribution as a function of data set size N (N given in the legend). In total 10^6 data points were drawn from a power-law distribution with exponent $\alpha=1.5$. [(b) and (c)] Similar distributions for power exponent estimators retrieved with (b) maximum likelihood estimation (MLE) and (c) logarithmically binned least-squares fitting (LBLS). Note that the largest two values of N in (a) are an order of magnitude larger than in (b) and (c) to highlight the persistent underestimation in LS estimators.

equal to t. In the lower panel of Fig. 3(b), the cumulative distribution of the $N=50$ data series used in Fig. 3(a) is given, together with the expected distributions for $\alpha=1.50$ and $\alpha=1.37$, respectively. As can be seen, the $\alpha=1.37$ result well reproduces the data cumulative distribution in the middle region. Here we find closely spaced bins with a single or few events and this is where the unequal distribution of statistical noise by the log-log transformation is manifested. For the statistically reliable first data points, as well as for the tail of the distribution, the $\alpha=1.37$ result deviates considerably from the data cumulative distribution. In contrast, the $\alpha=1.50$ result better represents the behavior at the low and high ends of the distribution. This is also apparent from the top panel in Fig. 3(b), where the difference Δ between the data cumulative distribution and both models is given. Whereas for $\alpha=1.37$ Δ is bound to positive values only, $\alpha=1.50$ gives a more evenly distributed difference with a smaller $\Delta_{\max}$, indicating a larger significance[32] for the correspondence between data and model: for $m=1.50$, we have $\Delta_{\max}=0.103$ with a significance of 64%, compared to $\Delta_{\max}=0.168$ with a significance of 14% for $m=1.37$. Thus, from the evolution of the cumulative distributions and Δ, we see that indeed the LS result is biased by the statistical noise in the bins with a low number of events.

The bias in the LS result can be overcome by applying a nonlinear binning scheme in the construction of the frequency histogram. In Fig. 4(c) we present the distribution of power exponents retrieved by performing a logarithmic binning of the data followed by least-squares fitting (LBLS) of the probability density. The distributions are, especially for low N, markedly asymmetric, but contrary to the LS results in Fig. 4(a), the distribution average approaches $m_{\mathrm{LBLS}}=1.5$ for all N. Comparing the distributions in Fig. 4(c) with the MLE results in Fig. 4(b) we can clearly see that the MLE distributions are not only symmetric around their mean value, but that these distributions are also markedly narrower than the distributions of the LBLS results. Thus, the MLE procedure appears to have smaller statistical error margins than the LS method.

In order to better illustrate the differences between MLE, LS, and LBLS results in Fig. 4, we directly compare the distributions of m_{MLE}, m_{LS}, and m_{LBLS} retrieved from evaluating 500 (MLE) and 5000 (LS, LBLS) data sets of $N=200$ data points each. This comparison is given in Fig. 5. The bias in the LS results is again clearly visible, while the MLE results are centered around $\alpha=1.50$. The LBLS removes the bias in the LS result, but maintains the asymmetry and width of the LS distribution. Thus, apart from a better convergence of MLE results towards the correct power exponent, the MLE results also have a reduced statistical error.

In Fig. 6, we show the average estimator as a function of data set size for both estimation procedures in red. Again, the bias in the LS results is clearly visible, and more importantly, it can be seen that with increasing data set size, the average power exponent estimator diverges from the actual model parameter $\alpha=1.50$. The use of logarithmic binning removes this underestimation and the LBLS average estimator shows slight deviations from $\alpha=1.50$, around 0.01 in magnitude, for all N investigated. In Fig. 4(c) we have seen that the distribution of m_{LBLS} estimators is asymmetric around the distribution maximum, especially for the smaller data set sizes. Here, we see that the LBLS distribution average closely reproduces the value of $\alpha=1.50$ even for small N, while in Fig. 4(c) the distribution maximum for, e.g., $N=50$

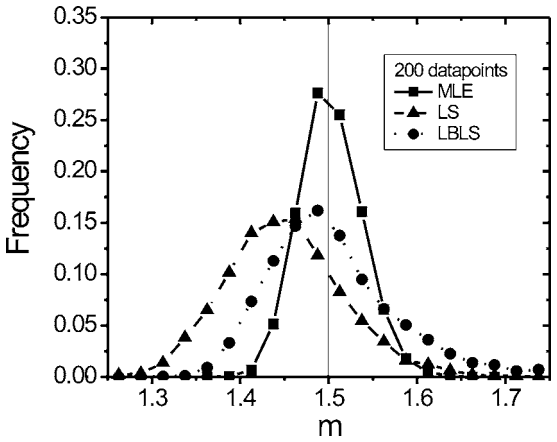

FIG. 5. Direct comparison of the distribution of power exponent estimators m retrieved with maximum likelihood estimation (MLE) (squares, solid line), least-squares fitting (LS) (triangles, dashed line), and logarithmically binned least-squares fitting (LBLS) (circles, dotted line) of data sets of size $N=200$ random numbers drawn from a power-law distribution with $\alpha=1.5$. The distribution of MLE estimators is considerably narrower and more symmetric around 1.5 compared to the LS and LBLS distributions. The distribution of LS estimators displays a clear underestimation.

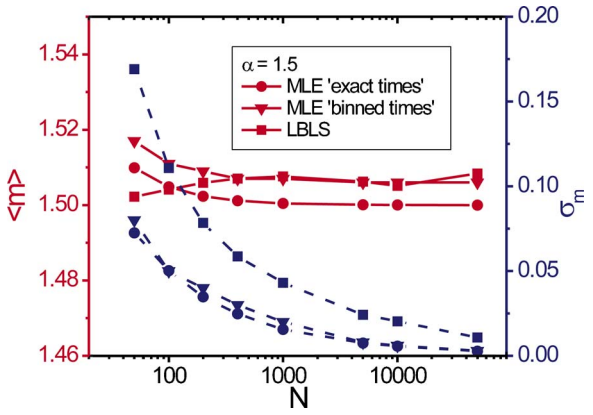

FIG. 7. (Color online) Comparison of the average power exponents (left axis and red solid lines) retrieved with the MLE procedure on series of binned times (down triangles) to the MLE result on exact times (circles), and the LBLS result (squares). As a result of binning, a slight, 0.01 overestimation compared to the "exact times" MLE results is introduced. This effect is comparable to the offset in the LBLS results. Standard deviation (right axis and blue dashed lines), or statistical error, of the exponents retrieved with MLE on "exact times" (circles) and "binned times" (down triangles) and with LBLS (squares).

is found to be around $m=1.41$. Thus the values retrieved with LBLS are spread over a wide range and, as we will see below, this indeed leads to a considerable statistical error in the LBLS result.

The average estimator retrieved with MLE on the other hand, rapidly and consistently converges towards 1.50 with increasing data set size. For data sets containing as few as 50 data points, the average exponent retrieved with MLE shows a slight, about 0.5%, deviation from the model value. This deviation is manifested as a slight overestimation, in line with the analytical result in Eq. (14). Apart from the fact that the overestimation is as small as 0.5% for $N=50$, we can also see in Fig. 6 as well as in Eq. (14) that it rapidly decreases to zero with increasing data set size. We will compare the numerical results in more detail to the analytical expressions in Eqs. (14) and (16) in Sec. V B. Here, we will focus on the comparison between MLE, LS, and LBLS procedures. Clearly, the MLE procedure constitutes a more reliable estimation technique for extracting power-law blinking exponents than LS fitting of the logarithmically transformed probability density.

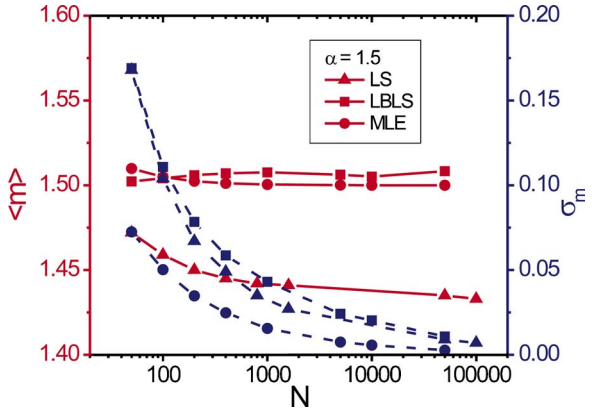

FIG. 6. (Color online) Average power exponents (left axis and red solid lines) retrieved with LS (triangles), LBLS (squares), and MLE (circles) as a function of the number of data points. The LS results show a persistent, diverging underestimation, whereas the MLE results converge to the underlying exponent of $\alpha=1.5$. Standard deviation (right axis and blue dashed lines), or statistical error, of the exponents retrieved with LS (triangles), LBLS (squares), and MLE (circles). The error margins in LS and LBLS procedures are comparable, while the MLE procedure yields considerably smaller error margins.

Apart from the average retrieved exponents, also indicated in Fig. 6 are the standard deviations of the distributions of m_{MLE}, m_{LBLS}, and m_{LS}. These constitute a measure for the statistical error in these procedures as a function of data set size. While we have seen before that the LBLS yields, on average, a more accurate estimation of the true power exponent than LS, here we see that the error in the m_{LBLS} values is similar to or larger than that in the m_{LS} values. For both these procedures the error margins are consistently two to three times larger than for the MLE procedure. With the MLE technique, we see that the result is already reliable up to the first decimal for data set size as small as $N=50$. Furthermore, we can see that the statistical error for m_{MLE} converges an order of magnitude in data set size faster to zero than for m_{LS}. Thus, we conclude that the MLE procedure is superior in retrieving the correct model exponent and reducing the statistical error involved in the estimation.

B. MLE accuracy and error margins

We now investigate the MLE accuracy in more detail. One of the advantages of the MLE procedure is that it can be performed directly on the "exact times" sequence, while the LS methods need additional binning in the construction of a probability density function. In practice, however, experimental data are binned by the time resolution t_{min} and this binning will influence the MLE.[29] We want to stress that this binning procedure is inherent to the experimental situation and that the LS and LBLS procedures would still need additional binning in construction of the probability density.

In Fig. 7, we present the results of MLE calculations on "binned times" sequences. The binned times MLE result is

seen to follow the same consistent convergent behavior upon increasing data set size as the exact times MLE but with a small additional overestimation. The deviation from the actual exponent $\alpha=1.5$ is comparable to the LBLS result. The statistical error in the binned times MLE result is, however, hardly affected by the binning and, thus, like the exact times MLE result, considerably smaller than with the LBLS procedure. As with the exact times result, the power exponent is already correctly estimated up to the first decimal for data set size of $N=50$.

Before, we have seen that the statistical error margins are particularly important for data set size below $N=1000$. All investigations thus far have been performed for power-law distributions with exponent $\alpha=1.5$. We will now investigate the accuracy and error margins of the MLE procedure as a function of the power exponent and compare the numerical results with the analytical expressions in Eqs. (14) and (16) derived before. For α ranging from 1.1 to 3.0, we have applied the same procedure as before and thus determined the distribution of retrieved exponents m_{MLE} for data set size $N=50$, 100, 200, and 400, respectively. First, we will focus on the results of exact times sequences.

The relative deviation of the average $\langle m \rangle$ with respect to α is depicted in Fig. 8(a). There is a small overestimation for almost all α that grows with increasing α, but this remains below 1.5% even for the smallest data set size of $N=50$. This overestimation is very well represented by Eq. (14), the results of which are indicated in Fig. 8(a) by the solid lines. When the number of data points increases to above 100, this overestimation rapidly decreases to below 0.5% for all α and thus becomes nearly negligible.

In Fig. 8(b), we show the relative full width at half maximum of the distribution of power exponent estimates, again as a function of both α and N. This provides a measure of the statistical error of the MLE procedure. We observe an increase of the relative error with increasing α, but again, the errors remain relatively small, below 10% for data set size as small as 50 points, and furthermore, rapidly decrease with growing data set size. Like the result for the overestimation of α, the statistical errors retrieved from our calculations smoothly follow the result obtained from Eq. (16), which is indicated by the solid lines. For the smallest value of α investigated, $\alpha=1.1$, we observe a slight increase in the statistical error for a larger data set size together with a deviant underestimation. This is probably due to the increased probability of observing events in the tail of the power-law distribution. In any case, for this α, the underestimation and the statistical error are, in absolute values, limited to -0.006 and 0.02, respectively, which will in general be negligible compared to measurement errors.

The results for binned times sequences are displayed in Fig. 9. With respect to the accuracy of the average estimator in Fig. 9(a), we again observe the overestimation of the power exponent due to the data binning. For values around $\alpha=1.5$ this overestimation remains relatively small, about 1% of the power exponent, and comparable to the analytical result for the exact times series. For increasing above $\alpha=1.6$ the overestimation in the binned times result grows more rapidly than for the exact times, but remains limited to

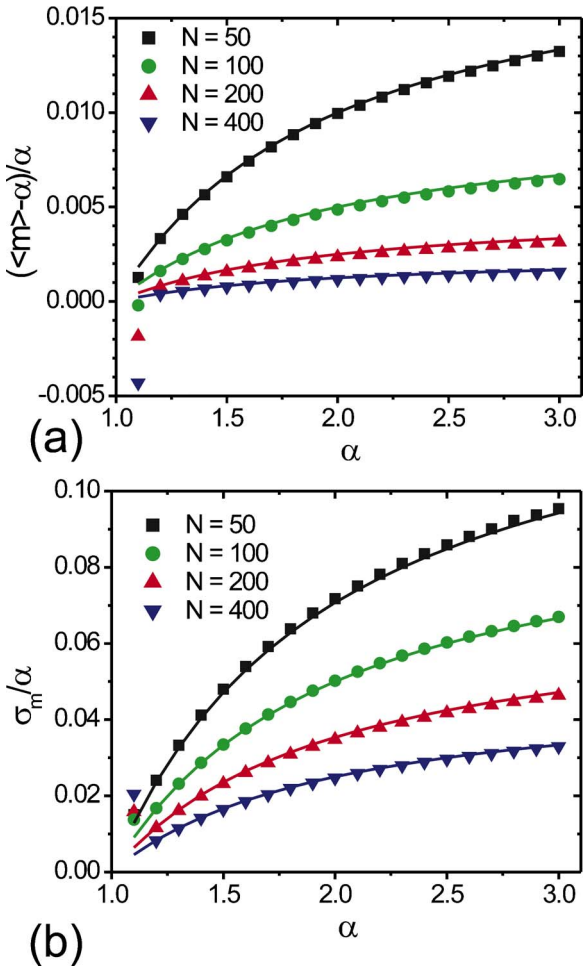

FIG. 8. (Color online) (a) Relative accuracy and (b) relative statistical error of the MLE procedure as a function of power-law exponent α for different data set sizes N. The results have been retrieved on data sets consisting of exact times. The graphs provide an estimate of the accuracy and the error margins of an estimated power exponent. The solid lines indicate the analytical results from Eqs. (14) and (16), respectively.

at maximum 3% for $\alpha=2$. With α rising above $\alpha=2$, this overestimation rapidly increases from about 8% for $\alpha=2.5$ up to almost 15% for $\alpha=3.0$. This behavior is intrinsic to the binning process as it is seen to be hardly dependent on the data set size. Regarding the power-law blinking of single emitters, most data and models reported so far indicate power exponents in between $\alpha=1.0$ and $\alpha=2.0$. The overestimation by MLE in this range remains below 3%, which is negligible compared to the bias in the LS estimator observed before and comparable to the fluctuating bias in the LBLS estimator.

Next, we turn to the relative statistical error in the binned times MLE results, which is depicted as a function of α in Fig. 9(b). Comparing the binned times results with the exact times results in Fig. 8(b), we can see that the two figures mainly differ for $\alpha>2.0$. For the exact times result we observed a flattening of the growth of σ_m/α in this region corresponding to the $(1-\alpha^{-1})$ dependency that results from Eq. (16), while for the binned times σ_m/α increases almost in linear dependency with α. For the range of $1.0<\alpha<2.0$, which is most relevant for blinking chromophores, however, the differences between the error margins of the exact times

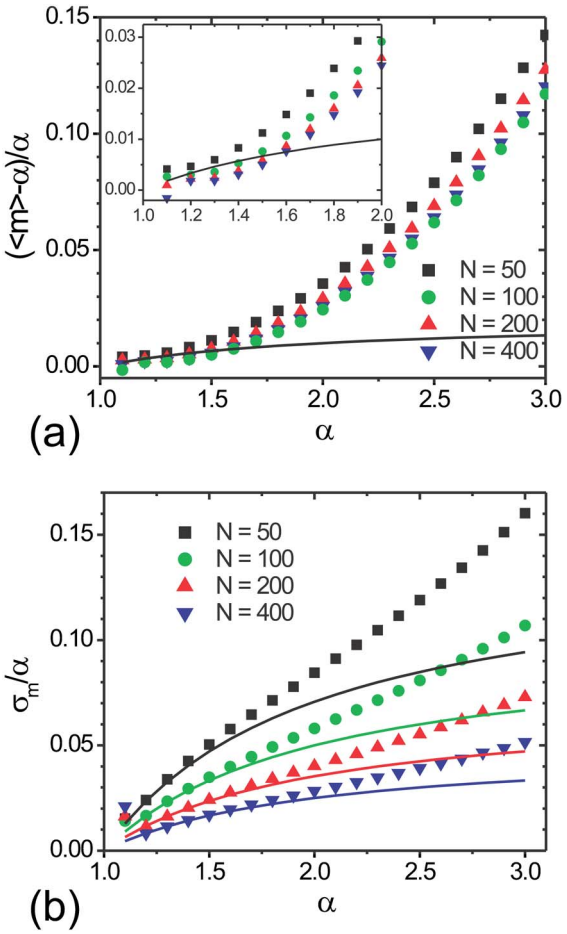

FIG. 9. (Color online) (a) Relative accuracy of the MLE procedure applied to sequences of binned times. The overestimation of the power exponent due to the use of binned times is persistent for each data set size and rapidly increases for $\alpha>2$. The black solid line indicates the theoretical result for "exact times" for $N=50$ [following Eq. (14)]. (b) Relative statistical error in the MLE procedure on binned times. The solid lines indicate the theoretical relative standard deviation [Eq. (16)] for exact times for $N=50$ (black), 100 (green), 200 (red), and 400 (blue). Compared to the exact times result, the statistical error is mostly affected by the binning procedure for $\alpha>2$.

estimator and the binned times estimator are negligble, corresponding to the observations for $\alpha=1.5$ in Fig. 7. For both exact times as well as for binned times, the relative standard deviation of the estimators remains below 8% for $N=50$ and below 5% for $N=200$. Thus, we see that the observations made for $\alpha=1.5$ on the accuracy and reliability of the MLE procedure hold for the range of $1.0<\alpha<2.0$ and can to good approximation be represented by the analytical expressions in Eqs. (14) and (16). Care should be taken for values $\alpha>2.0$, where the overestimation due to data binning as well as the statistical error margins rapidly increase and an assessment of their magnitude, as presented here, becomes indispensable in the interpretation of retrieved power exponents.

C. Assessment of power-law behavior

Finally, we want to note on the use of the maximum likelihood estimator derived in this paper and the assessment whether or not the data set actually obeys a power-law relationship. One of the aforementioned advantages of the MLE procedure is that the calculation given in Eq. (8) can be easily performed directly on the data set, contrary to LS procedures. However, this calculation will have an outcome for any underlying distribution and although many distributions will render results that are far off with respect to the expected range of power exponents ($\alpha\sim1.5$), the maximum likelihood estimator in itself does not prove whether or not data are actually distributed according to a power-law model. This can be illustrated with a single-exponential (SE) distribution $P(t)\sim e^{-\gamma t}$, for which it can be easily seen that Eq. (8) gives results around 1.5 if $\gamma\sim\frac{1}{3}$. The significance of the power-law behavior can be separately assessed by evaluation of the probability density, as in Fig. 3(a), or by applying a Kolmogorov-Smirnov test, as in Fig. 3(b). In the evaluation of a large amount of data sets these procedures, however, become quite laborious. Here, we want to present a simple mathematical procedure that in these circumstances can be applied to quickly detect possible deviations from the power-law model.

Taking a closer look at Eq. (8), we see that the last term on the right-hand side is equivalent to the expectation value $\langle\ln(t)\rangle$ over a power-law distribution, where $t=t_i/t_{\min}$ denotes the measured time scaled to the time resolution. Equivalently, we can derive expressions for the expectation values of a variety of other data functions, provided that these expectation values yield a finite result over the power-law distribution. An example of such a function is t^{-k}, for which we can derive

$$\langle t^{-k}\rangle=\frac{\int_1^\infty \tau^{-k}\tau^{-\alpha}d\tau}{\int_1^\infty \tau^{-\alpha}d\tau}=1-\frac{k}{k+\alpha-1}. \tag{18}$$

With Eq. (18) we find an estimator m_k for α that can be calculated by evaluating the expectation value $\langle t^{-k}\rangle$ over the data set,

$$m_k=1-k-\frac{k}{\langle t^{-k}\rangle-1}. \tag{19}$$

In the case of power-law behavior Eq. (19) gives a result comparable to m_{MLE}, while for other data distributions the m_k rapidly run to values an order of magnitude different from m_{MLE}. In Fig. 10 we show the average estimator $\langle m_k\rangle$ retrieved by evaluating 2000 random power-law distributed sequences of size $N=50$. For $k=0$ we list the result for $\langle m_{\mathrm{MLE}}\rangle$. The $\langle m_k\rangle$ on exact times sequences give results similar to $\langle m_{\mathrm{MLE}}\rangle$, and, in fact, the slight overestimation in the MLE result for $N=50$ is found to decrease for $\langle m_k\rangle$ with increasing k. This is due to the fact that the m_k estimator, because of its t^{-k} dependency, is less sensitive to undersampling in the tail of the distribution. For the binned times data series, the average m_k estimators for increasing k gradually rise with respect to the MLE result and we observe a similar behavior for the standard deviation, which rises to about 10% for $k=5$. For the exact times series, the behavior of the m_{MLE} with respect to the sequence of m_k provides a unique indication for power-law behavior: for other distributions, including the $\gamma=\frac{1}{3}$ SE distribution mentioned above, either the MLE result or the sequence of m_k estimators give widely differing values. For a SE distribution it can, e.g., be easily

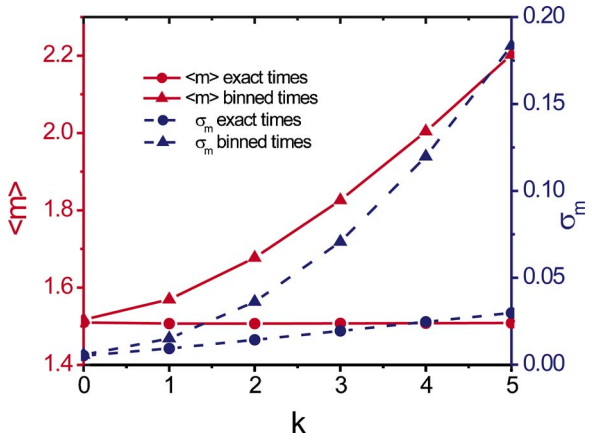

FIG. 10. (Color online) Results of the maximum likelihood estimator (at $k=0$) and the m_k estimators based on evaluation of $\langle t^{-k}\rangle$ following Eq. (13) applied to 2000 series consisting of $N=50$ data points. Average power exponents (left axis, red solid lines) and statistical errors (right axis, blue dashed lines) in the kth estimator on series of "exact times" are indicated with circles, whereas results on "binned times" with up triangles. For exact times, the m_k estimators give equivalent results as the MLE procedure. For binned times, there is an upward trend in the estimator with increasing error margins.

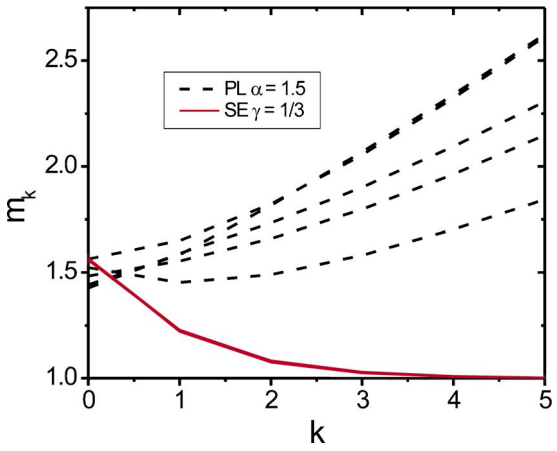

FIG. 11. (Color online) Result for the m_k estimators for five series each consisting of $N=50$ "binned" random numbers drawn from a power-law (PL) distribution with $\alpha=1.5$ (black dashed lines) and five series from a single-exponential (SE) distribution with $\gamma=1/3$ (red solid lines, all five curves fall on top of each other). At $k=0$ the MLE result is indicated. Despite the overlap in the MLE result for both distributions, the trend over the m_k estimators is markedly different. An increase in the values for the m_k estimators for k running from $k=0$ to $k=5$ of at maximum about +2.0 is indicative of power-law behavior.

seen that the sequence of m_k rapidly decays to $m_k=1$, irrespective of the value of m_{MLE}.

For the binned times, the situation more commonly encountered in experiments, the ability of the m_k estimators to detect power-law behavior is less straightforward because of the less consistent behavior of the sequence of m_k estimators and their increasing standard deviation observed in Fig. 10. Here, however, most distributions again show very different behavior from the typical power-law behavior illustrated in Fig. 10. In these situations, either m_{MLE} or the m_k sequence display values differing over an order of magnitude, while the power-law distribution shows an upward trend bounded approximately to $m_{\mathrm{MLE}}+1$. This bounded upward trend is illustrated in Fig. 11 for five different random "binned" data sets ($N=50$) for an $\alpha=1.5$ power law. Also indicated in Fig. 11 is the behavior of five random data sets from a SE distribution with $\gamma=\frac{1}{3}$. As can be seen, the MLE ($k=0$) results on both distributions are similar for all data sets. For the sequence of m_k estimators on the five SE distributed data sets, we observe a rapid and consistent decay to $m_k=1$ with increasing k for all data sets. This behavior is typical for SE distributions. The power-law data sets, on the other hand, show the typical rising behavior that was indicated by the averages in Fig. 10. Thus, calculation of a short sequence of m_k estimators together with the maximum likelihood estimator can serve as a fast check for the assumption of power-law behavior, without the need to evaluate the graphical appearance of a probability density. This can be particularly beneficial when large amounts of single-emitter data sets are to be evaluated, or when subsets in a large power-law distributed data set are to be evaluated, e.g., to check on dynamic effects or temporary transitions to single-rate, i.e., single-exponential, behavior.

Apart from deviations of the data distribution from power law to, e.g., SE, there may be physical constraints that limit the range of on- and off-time durations over which a power-law dependence can be observed. For instance, in the case of fluorescence blinking, fast triplet transitions, characterized by microseconds time scale SE kinetics,[3,11,12] will give deviations from power-law behavior at short time scales. For semiconductor nanocrystal blinking it has been reported that the on-time distribution can exhibit cutoff at large times.[7] If included in the data analysis, these phenomena will lead to erroneous results in the MLE procedure. Detection of these constraints still requires (visual) inspection of the on- and off-time probability densities and subsequent selection of the appropriate range over which power-law behavior is observed. With respect to short time scale triplet blinking, this can simply be done by applying a millisecond time scale binning to the intensity trace, thus averaging out all triplet kinetics (cf. Fig. 1).

VI. SUMMARY AND CONCLUSIONS

In this paper, we have analyzed the accuracy of estimation routines for extracting the power exponents from power-law distributed data such as single-emitter blinking times. Sequences of power-law distributed random numbers were generated and the power exponent was estimated by least-squares fitting of the log-log transformed probability density and by using a maximum likelihood procedure. We have demonstrated that least-squares fitting exhibits a severe underestimation of the actual power exponent. This underestimation can be circumvented by applying a logarithmic binning scheme prior to construction of the probability density or by using the maximum likelihood procedure. The maximum likelihood procedure already correctly predicts the power exponent for data set size as small as 50 numbers and was found to be superior in both estimating the correct power exponent as well as in reducing the statistical error. Furthermore, this procedure involves only a simple summa-

tion, given in Eq. (8), over the series of (power-law distributed) data points and can thus be performed in an easy and fast way.

For the maximum likelihood procedure, we have numerically and analytically investigated the accuracy and error margins of the estimation result as a function of both data set size and power exponent. For data consisting of "exact times," these results are displayed in Fig. 8, and the analytical expressions are given in Eqs. (14) and (16). We observed a very good correspondence between the numerical data and the analytical expressions. For a data set size as small as 50 numbers there is a slight overestimation of the power exponent, which increases when the exponent increases. This overestimation decays as $1/N$ with data set size N and its magnitude can be evaluated using Eq. (14). For $N=50$, the overestimation is less than 1% for power exponents in between $\alpha=1.0$ and $\alpha=2.0$, and becomes negligible when the data set size increases to above 100 numbers.

For "binned times," i.e., data limited by a finite experimental time resolution, the numerical results are displayed in Fig. 9. Using Eqs. (14) and (16), together with Figs. 8 and 9, the accuracy and error margins of experimentally obtained power exponent can be evaluated. For binned times there is an additional small overestimation of the power exponent by about 2% for all data set sizes, which rapidly increases for $\alpha>2.0$. The statistical error in the maximum likelihood result for $1.0<\alpha<2.0$ is below 8% for a data set size of only 50 numbers and decays further to below 5% for 200 numbers. For $\alpha<2.0$ the statistical error margins for binned data can to good approximation be evaluated using the exact times result of Eq. (16).

Using maximum likelihood estimation it should be readily possible to determine blinking exponents up to first decimal even when data set size is limited, e.g., due to photobleaching of organic fluorophores. Power-law blinking in the fluorescence of organic molecules has only recently been reported, its detection being seriously hindered by the low amount of observable long-time scale events before photobleaching. So far, data have been mainly analyzed by adding blinking data from multiple molecules.[9,12,20]

The maximum likelihood procedure presented here can be used to investigate this phenomenon at the level of single emitters.[36] Furthermore, given the relative error margins presented in Fig. 9(b), one can establish whether a distribution of exponents retrieved from several single emitters is homogeneous, i.e., exhibits a universal value of α, or is heterogeneous. Recently, there have been indications that in quantum dot blinking the on state is not adequately described by a simple one state picture, but rather consists of multiple or even a continuous distribution of on states characterized by different luminescence intensities and lifetime levels.[15,40] The different on states then result from different charge distributions surrounding the quantum dot. The multitude of on states then explains the power-law dependence observed when a simple two state on/off model is applied to the intensity trace. We want to note that it is this resulting power-law behavior that can be evaluated using the MLE procedure. Only when multiple levels can be unambiguously defined can the MLE procedure be applied to analyze the distribution of durations of each of these levels. Dynamic effects in the power-law distribution could be probed by applying the MLE procedure to small subsets in the intensity trace and comparing the width of the distribution of retrieved exponents to the calculated distributions presented here. Finally, we want to note that data in many other research areas exhibit power-law frequency distributions such as links and site sizes on the world wide web,[41] baby name giving,[42] human dynamics,[43] journal references,[44] and earthquake data.[45] The results presented above can be applied in the study of any system displaying power-law behavior.

ACKNOWLEDGMENTS

We would like to thank Robert Moerland for a critical reading of the manuscript. We are grateful to Jordi Hernando, Erik van Dijk, Maria García-Parajó, and Niek van Hulst for helpful and stimulating discussions. This work was supported by the Volkswagen Foundation, research priority area "Single Molecules" [to one of the authors (J.P.H.)].

[1] W. E. Moerner and M. Orrit, Science **283**, 1670 (1999); F. Kulzer and M. Orrit, Annu. Rev. Phys. Chem. **55**, 585 (2004); P. Tinnefeld and M. Sauer, Angew. Chem., Int. Ed. **44**, 2642 (2005).
[2] W. E. Moerner, Science **277**, 1059 (1997).
[3] T. Basche, S. Kummer, and C. Brauchle, Nature (London) **373**, 132 (1995).
[4] R. M. Dickson, A. B. Cubitt, R. Y. Tsien, and W. E. Moerner, Nature (London) **388**, 355 (1997).
[5] D. A. VandenBout, W. T. Yip, D. H. Hu, D. K. Fu, T. M. Swager, and P. F. Barbara, Science **277**, 1074 (1997).
[6] M. Kuno, D. P. Fromm, H. F. Hamann, A. Gallagher, and D. J. Nesbitt, J. Chem. Phys. **112**, 3117 (2000).
[7] K. T. Shimizu, R. G. Neuhauser, C. A. Leatherdale, S. A. Empedocles, W. K. Woo, and M. G. Bawendi, Phys. Rev. B **63**, 205316 (2001).
[8] R. G. Neuhauser, K. T. Shimizu, W. K. Woo, S. A. Empedocles, and M. G. Bawendi, Phys. Rev. Lett. **85**, 3301 (2000).
[9] J. P. Hoogenboom, E. M. H. P. van Dijk, J. Hernando, N. F. van Hulst, and M. F. Garcia-Parajo, Phys. Rev. Lett. **95**, 097401 (2005); J. Schuster, F. Cichos, and C. von Borczyskowski, Appl. Phys. Lett. **87**, 051915 (2005).
[10] R. J. Cook and H. J. Kimble, Phys. Rev. Lett. **54**, 1023 (1985).
[11] M. Orrit and J. Bernard, Phys. Rev. Lett. **65**, 2716 (1990); J. A. Veerman, M. F. Garcia-Parajo, L. Kuipers, and N. F. van Hulst, *ibid.* **83**, 2155 (1999); F. Kohn, J. Hofkens, R. Gronheid, M. Van der Auweraer, and F. C. De Schryver, J. Phys. Chem. A **106**, 4808 (2002); P. Tinnefeld, J. Hofkens, D.-P. Herten, S. Masuo, T. Vosch, M. Cotlet, S. Habuchi, K. Müllen, F. C. De Schryver, and M. Sauer, ChemPhysChem **5**, 1786 (2004); M. A. Kol'chenko, B. Kozankiewicz, A. Nicolet, and M. Orrit, Opt. Spectrosc. **98**, 681 (2005).
[12] M. Haase, C. G. Hübner, E. Reuther, A. Herrmann, K. Müllen, and T. Basche, J. Phys. Chem. B **108**, 10445 (2004).
[13] M. Kuno, D. P. Fromm, H. F. Hamann, A. Gallagher, and D. J. Nesbitt, J. Chem. Phys. **115**, 1028 (2001).
[14] W. van Sark, P. Frederix, A. A. Bol, H. C. Gerritsen, and A. Meijerink, ChemPhysChem **3**, 871 (2002).
[15] R. Verberk, A. M. van Oijen, and M. Orrit, Phys. Rev. B **66**, 233202 (2002).
[16] F. D. Stefani, W. Knoll, M. Kreiter, X. Zhong, and M. Y. Han, Phys. Rev. B **72**, 125304 (2005).
[17] R. Verberk, J. W. M. Chon, M. Gu, and M. Orrit, Physica E (Amsterdam) **26**, 19 (2005); A. Issac, C. von Borczyskowski, and F. Cichos, Phys. Rev. B **71**, 161302 (2005).
[18] X. Brokmann, J. P. Hermier, G. Messin, P. Desbiolles, J. P. Bouchaud, and M. Dahan, Phys. Rev. Lett. **90**, 120601 (2003).
[19] E. Lutz, Phys. Rev. Lett. **93**, 190602 (2004); G. Margolin and E. Barkai, *ibid.* **94**, 080601 (2005).
[20] E. K. L. Yeow, S. M. Melnikov, T. D. M. Bell, F. C. De Schryver, and J. Hofkens, J. Phys. Chem. A **110**, 1726 (2006).
[21] T. D. Krauss and L. E. Brus, Phys. Rev. Lett. **83**, 4840 (1999).

[22] R. Zondervan, F. Kulzer, S. B. Orlinskii, and M. Orrit, J. Phys. Chem. A **107**, 6770 (2003).
[23] J. Tang and R. A. Marcus, J. Chem. Phys. **123**, 054704 (2005).
[24] G. Margolin, V. Protasenko, M. Kuno, and E. Barkai, e-print cond-mat/0506512.
[25] M. Kuno, D. P. Fromm, S. T. Johnson, A. Gallagher, and D. J. Nesbitt, Phys. Rev. B **67**, 125304 (2003).
[26] I. S. Osad'ko, JETP Lett. **79**, 522 (2004).
[27] G. Messin, J. P. Hermier, E. Giacobino, P. Desbiolles, and M. Dahan, Opt. Lett. **26**, 1891 (2001); R. Verberk and M. Orrit, J. Chem. Phys. **119**, 2214 (2003).
[28] M. Pelton, D. G. Grier, and P. Guyot-Sionnest, Appl. Phys. Lett. **85**, 819 (2004).
[29] J. Tellinghuisen and C. W. Wilkerson, Anal. Chem. **65**, 1240 (1993).
[30] M. Maus, M. Cotlet, J. Hofkens, T. Gensch, F. C. De Schryver, J. Schaffer, and C. A. M. Seidel, Anal. Chem. **73**, 2078 (2001).
[31] M. L. Goldstein, S. A. Morris, and G. G. Yen, Eur. Phys. J. B **41**, 255 (2004).
[32] W. H. Press, S. A. Teukolsky, W. T. Vetterling, and B. P. Flannert, *Numerical Recipes in C: The Art of Scientific Computing*, 2nd ed. (Cambridge University Press, Cambridge, 1992).
[33] P. Hall and B. Selinger, J. Phys. Chem. **85**, 2941 (1981); C. Moore, S. P. Chan, J. N. Demas, and B. A. DeGraff, Appl. Spectrosc. **58**, 603 (2004).
[34] K. D. Osborn, M. K. Singh, R. J. B. Urbauer, and C. K. Johnson, ChemPhysChem **4**, 1005 (2003).
[35] D. A. Koster, C. H. Wiggins, and N. H. Dekker, Proc. Natl. Acad. Sci. U.S.A. **103**, 1750 (2006).
[36] J. P. Hoogenboom, J. Hernando, E. M. P. H. Van Dijk, N. F. van Hulst, and M. F. Garcia-Parajo (unpublished).
[37] F. D. Stefani, X. H. Zhong, W. Knoll, M. Y. Han, and M. Kreiter, New J. Phys. **7**, 197 (2005).
[38] M. Lippitz, F. Kulzer, and M. Orrit, ChemPhysChem **6**, 770 (2005).
[39] www.random.org
[40] K. Zhang, H. Chang, A. Fu, A. P. Alivisatos, and H. Yang, Nano Lett. **6**, 843 (2006).
[41] R. Albert, H. Jeong, and A.-L. Barabási, Nature (London) **401**, 130 (1999); B. A. Huberman and L. A. Adamic, *ibid.* **401**, 131 (1999).
[42] M. W. Hahn and R. A. Bentley, Proc. R. Soc. London, Ser. B **270**, S120 (2003).
[43] A.-L. Barabási, Nature (London) **435**, 207 (2005).
[44] S. Redner, Eur. Phys. J. B **4**, 131 (1998).
[45] P. Bak, K. Christensen, L. Danon, and T. Scanlon, Phys. Rev. Lett. **88**, 178501 (2002).